Analysis of surface relief diffraction gratings made of anisotropic material

Optical and Quantum Electronics **31:** 943–955, 1999.

Analysis of surface relief diffraction gratings made of anisotropic material

SERGIO BASTONERO, VITO LANCELLOTTI AND RENATO ORTA
Dipartimento di Elettronica, Politecnico di Torino, C.so Duca degli Abruzzi 24, 10129 Torino, Italy

Received 10 November 1998; accepted 8 February 1999

Abstract. A modal method for the analysis of surface relief gratings made with anisotropic material is presented. The structure is decomposed into a series of cascaded discontinuities between planar waveguides with stratified anisotropic dielectric. The basic problem is formulated by an integral equation which is solved numerically by the method of moments. The mode functions of the periodic region are assumed as basis functions to represent the unknown field on the junctions. Each junction is viewed as a waveguide junction problem and has been characterized by the generalized scattering matrix (GSM). The diffraction efficiencies of the grating are determined by combining the various GSM. In this way, the analysis method is stable and can be applied also to deep gratings.

Key words: anisotropic media, diffraction gratings, numerical methods

1. Introduction

Diffraction gratings are components of great interest for their various applications, for instance, in integrated optics, holography and spectroscopy (Gaylord and Moharam 1985). Usually, the dielectric is considered to be isotropic, but sometimes also anisotropic materials are used. Then it is important to develop a formalism to analyze these kinds of structures.

Among the methods introduced for the analysis of diffraction gratings, one can recall the integral method (Petit 1980), the coupled wave method (Gaylord and Moharam 1985; Chateau and Hugonin 1994) and the differential method (Montiel and Neviere 1994). Anisotropic gratings with modulated refraction index have been analyzed in (Glytsis and Gaylord 1987). Lamellar gratings were studied in (Mori *et al.* 1990) by the coupled wave method, but the convergence is slow, because the Fourier series is not appropriate to represent a discontinuous index profile.

In this paper, we discuss a modal method that is particularly suited for the analysis of dielectric relief diffraction gratings with steplike profile of the type shown in Fig. 1.

The approach, already used in the case of isotropic gratings (Orta *et al.* 1997), is to view the structure as the cascade of junctions between periodic arrays of slab waveguides with the same period and different heights. Each

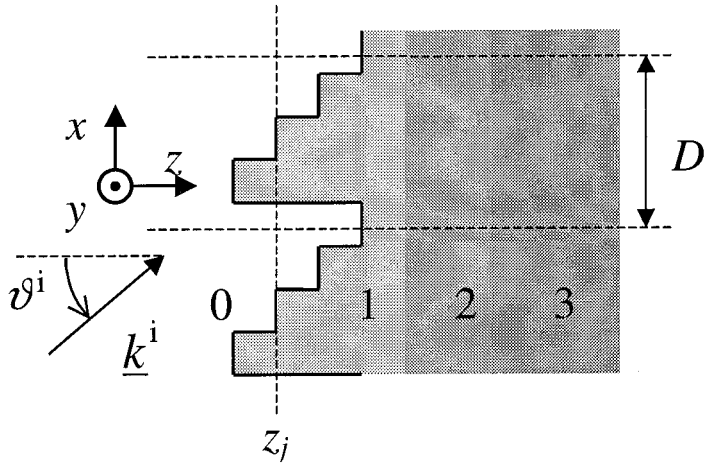

Fig. 1. Geometry of a lamellar surface relief diffraction grating.

junction is characterized by its Generalized Scattering Matrix (GSM) and the diffraction efficiencies of the grating are obtained by combining the various GSM according to the rules of circuit theory. The scattering matrix formalism is intrinsically stable and the well-known numerical problems which make difficult the analysis of deep gratings are avoided. See (Li 1996) for an extensive discussion of this issue.

2. Junction between two planar anisotropic dielectric guides

The main problem in the analysis of the grating of Fig. 1 is the characterization of the junction, at $z = z_j$, between two regions consisting of periodic arrays of dielectric slabs, with the same periodicity (lattice step D) but with different thickness. The incident field is assumed to be a plane wave with wavevector contained in the x, z plane, forming the angle ϑ^i with the z axis. The incident plane wave enforces the phase shift over the period $k_0 D n_0 \sin \vartheta^i$, where k_0 is the free space wavenumber and n_0 is refraction index of the medium from which the incident field comes. Thus the structure can be modelled as an inhomogeneously filled waveguide with phase shift walls (PSW) (see Fig. 2a).

This scattering problem can be formulated in terms of an integral equation, which is obtained by applying the Equivalence Theorem. The two regions are decoupled by introducing a perfectly conducting electric or magnetic plate, on which suitable magnetic or electric currents guarantee that the new problem is equivalent to the original one (Auda and Harrington 1983).

The boundary conditions require the continuity of the tangential electric and magnetic fields at the junction. In the case where a magnetic conductor is

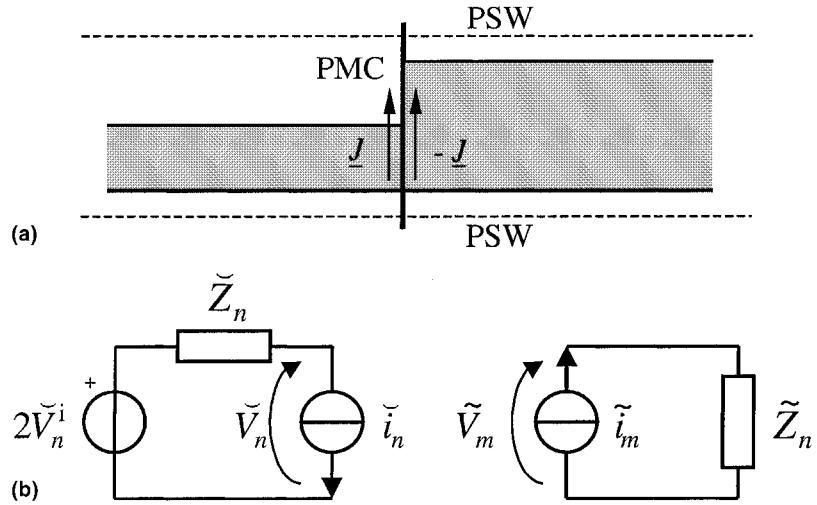

Fig. 2. Basic junction problem. (a) Application of the equivalence theorem. PMC: Perfect magnetic conductor. PSW: Phase shift wall. (b) Modal equivalent circuit.

introduced, the continuity of the magnetic field is ensured by assuming that the electric current distributions are opposite to each other on the two sides of the junction. Enforcing the continuity of the electric field leads to an integral equation that is termed electric field integral equation (EFIE). The unknown is the electric current distribution $\underline{J}(\underline{\rho}) = (-\hat{z}) \times \underline{H}_t(\underline{\rho}, z_j)$, that is essentially the transverse magnetic field at the junction. The kernel of the equation is the Green's function of the structure, which is easily derived in terms of the modes of the two waveguides. Fig. 2b shows the equivalent modal circuit (Felsen and Marcuvitz 1973, Ch. 2) of the junction. The superscripts $\breve{}$ and $\tilde{}$ are used to denote quantities relative to the left ($z < z_j$) and right region, respectively.

The keypoint in the application of the modal formalism is that the mode eigenfunctions form an orthonormal basis in the Hilbert space of transverse fields. As well known from general mathematical theorems, this happens only if the eigenproblem is self-adjoint, such as in the case of a lossless isotropic waveguide. If this condition is not satisfied, the mode eigenfunctions are not orthogonal and it becomes impossible to compute the field radiated by a given source distribution. On the other hand, it is always possible to construct an adjoint problem, whose eigenfunctions are orthogonal to those of the original problem, while the eigenvalues are the same (Felsen and Marcuvitz 1973, Ch. 8; Friedman 1965).

In the circuits shown in Fig. 2b, the unknown current generators $\breve{\imath}_n$ and $\tilde{\imath}_m$ are given by:

$$\breve{\imath}_n = \langle \underline{J}, \underline{\breve{e}}_n^+ \rangle \quad \tilde{\imath}_m = \langle \underline{J}, \underline{\tilde{e}}_m^+ \rangle \tag{1}$$

where the symbol $\langle .,. \rangle$ denotes a symmetrical inner product. In general, $\underline{e}_i^+$ is the electric field eigenfunction corresponding to the adjoint problem. In this work, we consider only the case of transverse anisotropy (i.e. the anisotropy is confined in the xy plane only). Then the waveguide with anisotropic dielectric has a reflection symmetry. The propagation constants can be real, imaginary or also complex, even for lossless dielectric (Felsen and Marcuvitz 1973, Ch. 8). The adjoint problem is obtained by substituting all the dyadic permittivities and permeabilities with their transpose. The modes of the two problems are identified by the common propagation constant k_{zi}. For the modes with real or imaginary propagation constant k_{zi}, the eigenfunction $\underline{e}_i^+$ is just the complex conjugate of $\underline{e}_i$, the eigenfunction of the original problem with the same propagation constant. The case of complex modes is more complicated. In fact they appear in four-tuples with propagation constants in the form $k_z = \pm\beta \pm j\alpha$. Among them, those with $k_z = \pm\beta - j\alpha$ are the progressive modes. Let $\underline{e}_{c1}$ be the electric field eigenfunction relative to the mode with propagation constant $k_z = \beta - j\alpha$ and let $\underline{e}_{c2}$ be the eigenfunction with $k_z = -\beta - j\alpha$, then one has

$$\underline{e}_{c1}^+ = \underline{e}_{c2}^* \quad \underline{e}_{c2}^+ = \underline{e}_{c1}^* \tag{2}$$

These rules hold in the lossless case and are derived by standard analytical techniques.

It is well-known that the choice of modal impedance is only a convention. The definition that will be used here for the case of an anisotropic guide, which generalizes the well-known choice for TE and TM modes, is based on the condition

$$\langle \underline{e}_n, \underline{e}_n^+ \rangle = \langle \underline{h}_n, \underline{h}_n^+ \rangle \tag{3}$$

i.e. the electric and magnetic field eigenfunctions have the same norm.

The voltage generator $2\check{V}_n^i$ accounts for the incident field and is computed via

$$\check{V}_n^i = \langle \underline{\check{E}}_t^i, \underline{\check{h}}_n^+ \times \hat{z} \rangle \tag{4}$$

The electric field on the two sides of the junction is computed easily from the modal circuit of Fig. 2:

$$\underline{\check{E}}_t = \sum_n \check{V}_n \underline{\check{e}}_n = \sum_n (2\check{V}_n^i - \check{\imath}_n \check{Z}_n) \underline{\check{e}}_n \tag{5}$$

$$\underline{\tilde{E}}_t = \sum_m \tilde{V}_m \underline{\tilde{e}}_m = \sum_m \tilde{\imath}_m \tilde{Z}_m \underline{\tilde{e}}_m \tag{6}$$

The boundary condition to be enforced requires that

$$\underline{\check{E}}_t(\underline{\rho}) - \underline{\tilde{E}}_t(\underline{\rho}) = 0 \quad \forall \underline{\rho} \tag{7}$$

This equation, by the substitution of (1–6), can be rewritten as the following EFIE:

$$\int \underline{\underline{G}}^E(\underline{\rho}, \underline{\rho}') \cdot \underline{J}(\underline{\rho}') \mathrm{d}\underline{\rho}' = 2\underline{\check{E}}_t^i(\underline{\rho}) \quad \forall \underline{\rho} \tag{8}$$

where the kernel (electric Green's function) is given by the following eigenfunction expansion:

$$\underline{\underline{G}}^E(\underline{\rho}, \underline{\rho}') = \sum_n \check{Z}_n \underline{\check{e}}_n(\underline{\rho}) \underline{\check{e}}_n^+(\underline{\rho}') + \sum_m \tilde{Z}_m \underline{\tilde{e}}_m(\underline{\rho}) \underline{\tilde{e}}_m^+(\underline{\rho}') \tag{9}$$

As remarked above, the equivalence theorem can also be applied in a different way, by inserting an electric plane in $z = z_j$. The unknown, in this case, is the equivalent magnetic current distribution $\underline{M}(\underline{\rho})$ introduced on the two sides of the junction (with opposite signs, so that the continuity of the electric field is guaranteed). Enforcing the continuity of the tangential magnetic field yields a magnetic field integral equation (HFIE), dual of (8):

$$\int \underline{\underline{G}}^H(\underline{\rho}, \underline{\rho}') \cdot \underline{M}(\underline{\rho}') \mathrm{d}\underline{\rho}' = 2\underline{\check{H}}_t^i(\underline{\rho}) \quad \forall \underline{\rho} \tag{10}$$

where the magnetic Green's function is computed through the following eigenfunction expansion:

$$\underline{\underline{G}}^H(\underline{\rho}, \underline{\rho}') = \sum_n \check{Y}_n \underline{\check{h}}_n(\underline{\rho}) \underline{\check{h}}_n^+(\underline{\rho}') + \sum_m \tilde{Y}_m \underline{\tilde{h}}_m(\underline{\rho}) \underline{\tilde{h}}_m^+(\underline{\rho}') \tag{11}$$

which is derived from a modal circuit dual of that of Fig. 2. Note that (8) and (10) are just two examples; other integral equations can be obtained by applying the equivalence theorem in different forms.

Let us apply the method of moments to the solution of the EFIE (8). Let $\{\underline{f}_k(x)\}$ be a set of suitable basis functions: a small number of them must be capable of approximating accurately the unknown according to

$$\underline{J}(x) = \sum_k x_k \underline{f}_k(x) \tag{12}$$

Moreover, let $\{\underline{w}_l(x)\}$ be a set of suitable test functions, i.e. such that a small number of them can span the range of the linear operator. It is convenient to introduce a matrix formalism:

$$\check{F}_{nk} = \langle \underline{f}_k, \underline{\check{e}}_n^+ \rangle \quad \check{W}_{nl} = \langle \underline{w}_l, \underline{\check{e}}_n \rangle \tag{13}$$

$$\tilde{F}_{nk} = \langle \underline{f}_k, \underline{\tilde{e}}_n^+ \rangle \quad \tilde{W}_{nl} = \langle \underline{w}_l, \underline{\tilde{e}}_n \rangle \tag{14}$$

Then, the linear system derivable from (8) takes the form:

$$\left[\underline{\underline{\check{W}}}^T \cdot \underline{\underline{\check{Z}}} \cdot \underline{\underline{\check{F}}} + \underline{\underline{\tilde{W}}}^T \cdot \underline{\underline{\tilde{Z}}} \cdot \underline{\underline{\tilde{F}}} \right] \cdot \underline{x} = 2 \underline{\underline{\check{W}}}^T \cdot \underline{\check{V}}^i \tag{15}$$

where $\underline{\underline{\check{Z}}}$ and $\underline{\underline{\tilde{Z}}}$ are the diagonal matrices of the modal impedances. Let us denote by $\underline{\underline{Q}}$ the inverse of the coefficient matrix:

$$\underline{\underline{Q}} = \left[\underline{\underline{\check{W}}}^T \cdot \underline{\underline{\check{Z}}} \cdot \underline{\underline{\check{F}}} + \underline{\underline{\tilde{W}}}^T \cdot \underline{\underline{\tilde{Z}}} \cdot \underline{\underline{\tilde{F}}} \right]^{-1} \tag{16}$$

Then the electric current at $z = z_j$ is known through the coefficients of the basis functions:

$$\underline{x} = 2 \underline{\underline{Q}} \cdot \underline{\underline{\check{W}}}^T \cdot \underline{\check{V}}^i \tag{17}$$

The most convenient way to characterize the junction between the two arrays of dielectric waveguides is to use the GSM, i.e. the one referred to both propagating and cut-off modes. This can be computed easily on the basis of the circuits of Fig. 2. In fact, the scattered voltages are given by

$$\check{V}_n^s = \check{V}_n^i - \check{Z}_n \check{\imath}_n \quad \tilde{V}_m^s = \tilde{Z}_m \tilde{\imath}_m \tag{18}$$

and noting that

$$\check{\imath}_n = \sum_k \check{F}_{nk} x_k \quad \tilde{\imath}_m = \sum_k \tilde{F}_{mk} x_k \tag{19}$$

we obtain

$$\underline{\check{V}}^s = 2 \underline{\check{V}}^i - 2 \underline{\underline{\check{Z}}} \cdot \underline{\underline{\check{F}}} \cdot \underline{\underline{Q}} \cdot \underline{\underline{\check{W}}}^T \cdot \underline{\check{V}}^i \tag{20}$$

$$\underline{\tilde{V}}^s = 2 \underline{\underline{\tilde{Z}}} \cdot \underline{\underline{\tilde{F}}} \cdot \underline{\underline{Q}} \cdot \underline{\underline{\check{W}}}^T \cdot \underline{\check{V}}^i \tag{21}$$

If we now proceed in the same way as before by assuming a right-hand side incidence $\underline{\tilde{V}}^i$, we derive the GSM of the junction:

$$\begin{bmatrix} \underline{\check{V}}^s \\ \underline{\tilde{V}}^s \end{bmatrix} = \begin{bmatrix} \underline{\underline{S}}_{11} & \underline{\underline{S}}_{12} \\ \underline{\underline{S}}_{21} & \underline{\underline{S}}_{22} \end{bmatrix} \cdot \begin{bmatrix} \underline{\check{V}}^i \\ \underline{\tilde{V}}^i \end{bmatrix} \tag{22}$$

where

$$\begin{aligned}
\underline{\underline{S}}_{11} &= \underline{\underline{1}} - 2\,\underline{\underline{\check{Z}}} \cdot \underline{\underline{\check{F}}} \cdot \underline{\underline{Q}} \cdot \underline{\underline{\check{W}}}^T \\
\underline{\underline{S}}_{12} &= 2\,\underline{\underline{\check{Z}}} \cdot \underline{\underline{\check{F}}} \cdot \underline{\underline{Q}} \cdot \underline{\underline{\tilde{W}}}^T \\
\underline{\underline{S}}_{21} &= 2\,\underline{\underline{\tilde{Z}}} \cdot \underline{\underline{\tilde{F}}} \cdot \underline{\underline{Q}} \cdot \underline{\underline{\check{W}}}^T \\
\underline{\underline{S}}_{22} &= \underline{\underline{1}} - 2\,\underline{\underline{\tilde{Z}}} \cdot \underline{\underline{\tilde{F}}} \cdot \underline{\underline{Q}} \cdot \underline{\underline{\tilde{W}}}^T
\end{aligned} \tag{23}$$

The procedure for the solution of the HFIE (10) is very similar and will not be reported in detail. In this case, the basis functions are chosen to expand the magnetic current distribution. The elements of the GSM of the same junction, according to the HFIE formulation can be shown to be

$$\begin{aligned}
\underline{\underline{S}}_{11} &= 2\,\underline{\underline{\check{F}}} \cdot \underline{\underline{Q}} \cdot \underline{\underline{\check{W}}}^T \cdot \underline{\underline{\check{Y}}} - \underline{\underline{1}} \\
\underline{\underline{S}}_{12} &= 2\,\underline{\underline{\check{F}}} \cdot \underline{\underline{Q}} \cdot \underline{\underline{\tilde{W}}}^T \cdot \underline{\underline{\tilde{Y}}} \\
\underline{\underline{S}}_{21} &= 2\,\underline{\underline{\tilde{F}}} \cdot \underline{\underline{Q}} \cdot \underline{\underline{\check{W}}}^T \cdot \underline{\underline{\check{Y}}} \\
\underline{\underline{S}}_{22} &= 2\,\underline{\underline{\tilde{F}}} \cdot \underline{\underline{Q}} \cdot \underline{\underline{\tilde{W}}}^T \cdot \underline{\underline{\tilde{Y}}} - \underline{\underline{1}}
\end{aligned} \tag{24}$$

where the matrix $\underline{\underline{Q}}$ is defined in this case by

$$\underline{\underline{Q}} = \left\{ \underline{\underline{\check{W}}}^T \cdot \underline{\underline{\check{Y}}} \cdot \underline{\underline{\check{F}}} + \underline{\underline{\tilde{W}}}^T \cdot \underline{\underline{\tilde{Y}}} \cdot \underline{\underline{\tilde{F}}} \right\}^{-1} \tag{25}$$

and the matrices $\underline{\underline{F}}$ and $\underline{\underline{W}}$ are defined by equations similar to (13) with the electric field eigenfunctions $\underline{e}_i$ substituted with the magnetic field ones $\underline{h}_i$.

The determination of the modes of the various regions composed of arrays of dielectric slabs, which is necessary for the computation of the relevant Green's function, would require, as well known, the solution of a transcendental equation. To implement a fully automated procedure is not a trivial task, in particular, in the case of lossy dielectrics or when modes are almost degenerated. Thus, a different approach has been taken, i.e. the so called "tau method" of Lanczos (Orszag and Gottlieb 1977; and Lancellotti and Orta 1997). The wave equation is converted into an algebraic eigenvalue problem by introducing a suitable basis for the representation of the unknown. Since the modal fields have discontinuous derivatives at the dielectric interfaces, it is particularly convenient to use a piecewise Legendre polynomial basis, which provides exponential convergence rate. By exploiting the analytical properties of the representation, it is possible to determine the number of

basis polynomials to be employed for the determination of a certain eigenvalue with a prescribed accuracy (Lancellotti and Orta 1997).

A key point in the actual application of the method of moments is the selection of appropriate expansion and testing functions. For the numerical evaluation of the junction GSM given by (22), it is clear that one has to use a finite number of basis and test functions, as well as a finite number of modes in the two regions to represent the Green's function. As is well known, these numbers cannot be chosen independently but are related because of the relative convergence phenomenon (Mittra *et al.* 1972). The number of expansion functions, and hence the size of the matrix to be inverted, can be small thanks to a careful choice of them.

The modes of the two regions adjacent to the junction play roles that it is convenient to keep distinct. On the one hand, the modes are the ports with respect to which the junction GSM is defined, and their number depends on the accuracy with which the interaction with the adjacent discontinuities is to be described. On the other hand, the modes are used to represent the Green's function of the problem (see (9, 11)), and hence, the accuracy of the solution of the junction problem grows with the number of modes employed to evaluate the matrices $\underline{\underline{Q}}$ defined in (16) and (25).

A criterion that may be employed to decide the number of modes in order to have a good solution of the integral equation is based on the spatial bandwidth concept. The spatial bandwidth of the Green's function modal representation has to be larger than that of the aperture field in terms of expansion functions. In any case, the number of modes must be larger than the number of expansion function, otherwise the linear system matrix defined in (16) is singular.

3. Grating analysis

According to the strategy indicated in the introduction, the grating is decomposed into a series of junctions, each of which is characterized by its GSM. The GSM of the complete structure is computed by the cascade combination of the various GSM, also known as Redheffer star product, (Redheffer 1961). In the case of two junctions, with $(n+k)\times(n+k)$ scattering matrix $\underline{\underline{S}}'$ and $(k+m)\times(k+m)$ scattering matrix $\underline{\underline{S}}''$, when the k intermediate ports are connected, a structure with $n+m$ ports is obtained whose $(n+m)\times(n+m)$ matrix $\underline{\underline{S}}$ is obtained via

$$\begin{bmatrix} \underline{\underline{S}}_{11} & \underline{\underline{S}}_{12} \\ \underline{\underline{S}}_{21} & \underline{\underline{S}}_{22} \end{bmatrix} = \begin{bmatrix} \underline{\underline{S}}'_{11} & \underline{\underline{S}}'_{12} \\ \underline{\underline{S}}'_{21} & \underline{\underline{S}}'_{22} \end{bmatrix} * \begin{bmatrix} \underline{\underline{S}}''_{11} & \underline{\underline{S}}''_{12} \\ \underline{\underline{S}}''_{21} & \underline{\underline{S}}''_{22} \end{bmatrix} \tag{26}$$

where

$$
\begin{aligned}
\underline{\underline{S}}_{11} &= \underline{\underline{S}}'_{11} + \underline{\underline{S}}'_{12} \cdot \underline{\underline{S}}''_{11} \cdot \left(\underline{\underline{1}} - \underline{\underline{S}}'_{22} \cdot \underline{\underline{S}}''_{11}\right)^{-1} \cdot \underline{\underline{S}}'_{21} \\
\underline{\underline{S}}_{12} &= \underline{\underline{S}}'_{12} \cdot \left(\underline{\underline{1}} - \underline{\underline{S}}''_{11} \cdot \underline{\underline{S}}'_{22}\right)^{-1} \cdot \underline{\underline{S}}''_{12} \\
\underline{\underline{S}}_{21} &= \underline{\underline{S}}''_{21} \cdot \left(\underline{\underline{1}} - \underline{\underline{S}}'_{22} \cdot \underline{\underline{S}}''_{11}\right)^{-1} \cdot \underline{\underline{S}}'_{21} \\
\underline{\underline{S}}_{22} &= \underline{\underline{S}}''_{22} + \underline{\underline{S}}''_{21} \cdot \left(\underline{\underline{1}} - \underline{\underline{S}}'_{22} \cdot \underline{\underline{S}}''_{11}\right)^{-1} \cdot \underline{\underline{S}}'_{22} \cdot \underline{\underline{S}}''_{12}
\end{aligned}
\tag{27}
$$

where the partition of the various matrices is induced by the integers n, k, m.

In adopting this approach, it is extremely convenient to subdivide the modes on the two sides of a junction into two classes: *accessible modes* (Rozzi 1973) are those (above and below cut-off) that effectively contribute to the coupling with the adjacent discontinuity located at a distance s apart because their attenuation over s is less than a specified threshold; *localized modes* are the cut-off modes that are so attenuated that they do not interact with the neighbouring discontinuities and contribute just to reactive energy storing. Clearly, in the combination process, only the ports corresponding to the accessible modes are to be connected and this results often in the inversion of very small matrices.

It is to be remarked, furthermore, that this procedure is absolutely stable and accurate from a numerical point of view. The well-known problems encountered in the analysis of deep gratings were due to the fact that a formulation based on the multiplication of the junction's transmission matrices was used. In the presence of modes with high attenuation, even if overflow does not occur, linear dependence between the columns of the transmission matrices is introduced because of the finite arithmetic, which prevents from obtaining the grating efficiencies.

4. Numerical results

The formulation described by (10) is used to analyze the grating showed in Fig. 3, consisting of KH_4AsO_4 bars embedded in an isotropic substrate ($\varepsilon_2 = 2.25$) and covered with an isotropic layer ($\varepsilon_1 = 2.3$, $h_s = 2\,\mu\text{m}$). The crystal is uniaxial with ordinary refraction index $n_o = 1.570$ and extraordinary refraction index $n_e = 1.470$, with optical axis in the xy-plane and rotated through an angle $\alpha = 30^\circ$ from the x-axis. Then, in the xyz-reference, the relative permittivity for the material is described by the matrix

$$
\varepsilon_a = \begin{pmatrix} 2.2370 & 0.1316 & 0 \\ 0.1316 & 2.389 & 0 \\ 0 & 0 & 2.465 \end{pmatrix} \tag{28}
$$

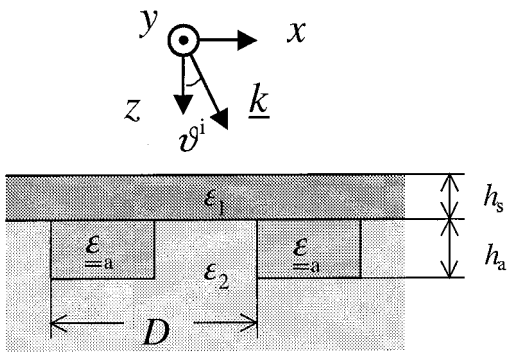

Fig. 3. Geometry of grating with $D = 0.44\,\mu m$, $\varepsilon_1 = 2.3$, $\varepsilon_2 = 2.25$, $h_s = 2\,\mu m$, $\vartheta = 32.189°$, $\lambda = 0.44\,\mu m$. For the anisotropic material $n_o = 1.570$, $n_e = 1.470$, $\alpha = 30°$.

The grating period is 0.44 μm and the duty-cycle is 50%. The incident field is a plane-wave from air with an incidence angle $\vartheta^i = 32.189°$, TE polarization (with respect to z axes) and wavelength $\lambda = 0.44\,\mu m$.

In this work, the modal eigenfunctions of the periodic region are selected as expansion and test functions. Therefore, the solution method is essentially the mode-matching method (Auda and Harrington 1983). All the elements of projection matrix can be calculated analytically, without the use of numerical integration.

The relative error on the energy conservation is of the order of 10^{-13}. Note, however, that even though some authors use this parameter to check the accuracy of the solution, with this formulation, the conservation of the complex power at the junction is automatically guaranteed, independently of the number of basis functions and of the number of terms in the modal expansion of the Green's function. Thus an energy conservation error at the roundoff level is a check of the correct software implementation of the solution technique, but nothing more.

The accuracy of the solution is checked instead by the graph of Fig. 4, which shows the plots of the total magnetic field on the two sides of the third junction, reconstructed in terms of the relevant modes of the two regions (periodic structure and uniform dielectric). The grating thickness is $h_a = 0.5\,\mu m$, whereas 9 modes of the periodic structure are used to expand the electric field on the junction and 11 modes to represent the Green function. The number of accessible modes (with attenuation over the distance to the adjacent discontinuity less than 30 dB) is 8. The good agreement of the two plots shows that the integral equation (10) is actually satisfied.

Finally, it is to be noted that the diffraction efficiencies are the parameters of interest to characterize the grating. It is possible to show that they are variational quantities, so that they suffer from only second order errors when the current distribution contains first order errors.

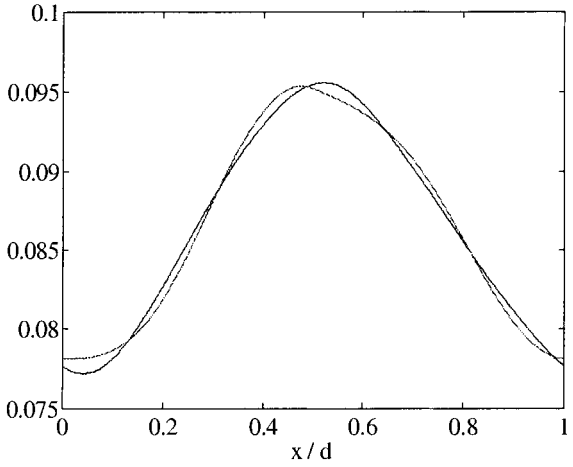

Fig. 4. Magnetic fields on the two sides of the third junction.

Figure 5 shows the transmission efficiencies for the 0 and -1 order and for TE and TM polarization when the grating depth h_a is varied. It can be noted that for increasing h_a, the conversion of power from TE to TM polarization also increases. The rapid oscillations of the efficiency curves have a period of the order of π/k_{z0} where k_{z0} is the propagation constant of the fundamental mode in the grating region. This is a phenomenon similar to that taking place in Fabry–Perot interferometers. However, in this case, the two discontinuities that define the interferometer (junction between homogenous and periodic dielectric) interact through 7 propagating modes.

Figure 6 shows the relative error on the reflection efficiencies for TE_0 and TE_{-1} order when the number of expansion functions used to represent the

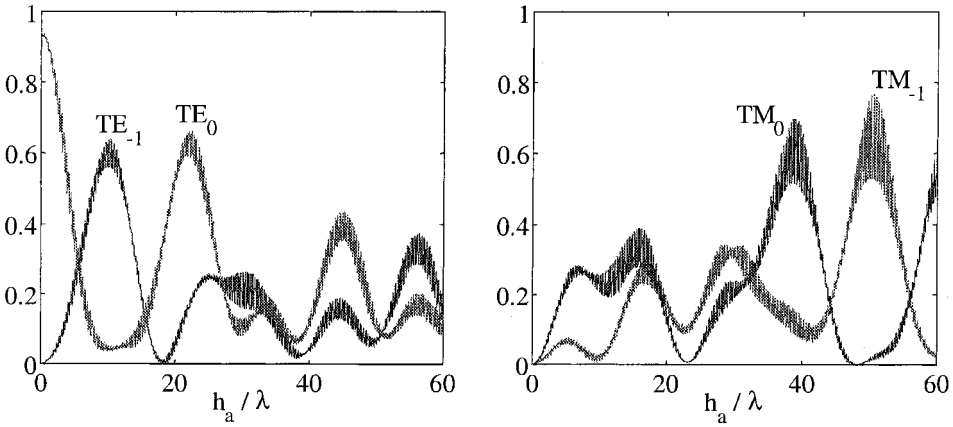

Fig. 5. Transmission efficiencies for TE_0, TE_{-1}, TM_0 and TM_{-1} with $\lambda = 0.44\,\mu m$.

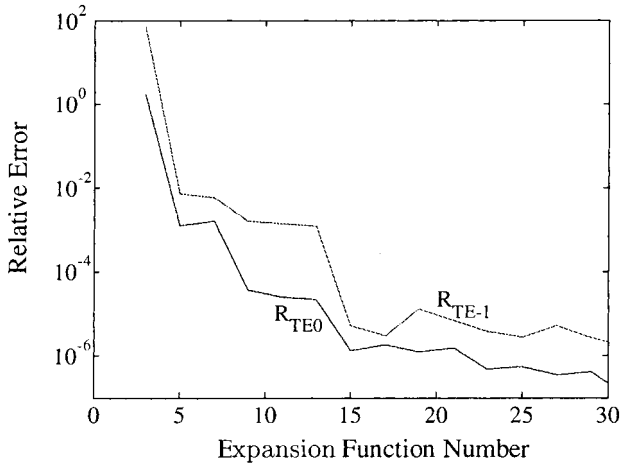

Fig. 6. Relative error on the reflection efficiencies vs expansion function number.

electric field at the junction is varied. The efficiencies obtained with 41 expansion functions are considered as reference. It can be noted that even with a small number of basis functions, the efficiencies have a good accuracy and this confirms the variational characteristics of efficiencies.

5. Conclusion

In this paper, a modal method has been presented for the analysis of lamellar surface relief dielectric gratings made by anisotropic material. The structure is decomposed into a series of successive discontinuities. Each of them is viewed as a waveguide junction problem and its generalized scattering matrix has been computed by solving an integral equation. The diffraction efficiencies of the gratings are determined by combining the various GSM. In this way, the analysis method is stable and can be applied also to deep gratings. The results presented refer to an incident plane wave with wavevector lying in the x,z plane. The extension to the general case of conical mounting is straightforward and is currently under way.

References

Auda, H. and R.F. Harrington. *IEEE Trans. Microwave Theory Tech.* **MTT-31** 515, 1983.
Chateau, N. and J. Hugonin. *J. Opt. Soc. Am. A* **11** 1321, 1994.
Felsen, L.B. and N. Marcuvitz. *Radiation and scattering of waves*, Prentice-Hall Inc., Englewood Cliffs, NJ, 1973.
Friedman, B. *Principles of Applied Math*, John Wiley & Sons, NY, Chapter 4, 1965.
Gaylord, T.K. and M.G. Moharam. *Proc. IEEE* **73** 894, 1985.

Glytsis, E.N. and T.K. Gaylord. *J. Opt. Soc. Am. A* **4** 2061, 1987.
Lancellotti, V. and R. Orta. In *Proceedings of the ICEAA 1997 Torino*, 33, 1997.
Li, L. *J. Opt. Soc. Am. A* **13** 1024, 1996.
Mittra, R., T. Itoh and T. Li. *IEEE Trans. on Microwave Theory Tech.* **MTT-20** 96, 1972.
Montiel, F. and M. Neviere. *J. Opt. Soc. Am. A* **11** 3241, 1994.
Mori, S., K Mukai, J. Yamakita and K. Rokushima. *J. Opt. Soc. Am. A* **7** 1661, 1990.
Orszag, S.A. and D. Gottlieb. *Numerical Analysis of Spectral Methods: Theory and Applications*, 37, SIAM Philadelphia, 1977.
Orta, R., S. Bastonero and R. Tascone. In *Diffractive Optics and Optical Microsystems*, eds S. Martellucci and A. Chester, 47, Plenum, 1997.
Petit, R. ed. *Electromagnetic Theory of Gratings*, Springer-Verlag, Berlin, 1980.
Redheffer, R. In *Difference and functional equations in transmission line theory in Modern Mathematics for the Engineer*, ed. E.F. Beckenbach McGraw-Hill, New York, 1961.
Rozzi, T.E. *Int. J. Circuit Theory and Appl.* **1** 161, 1973.